Available online at www.sciencedirect.com
SCIENCE DIRECT®
Bioorganic & Medicinal Chemistry 12 (2004) 4917–4927
Bioorganic & Medicinal Chemistry

Angiogenesis inhibitor TX-1898: syntheses of the enantiomers of sterically diverse haloacetylcarbamoyl-2-nitroimidazole hypoxic cell radiosensitizers

Cheng-Zhe Jin,[a,f] Hideko Nagasawa,[a] Mariko Shimamura,[b] Yoshihiro Uto,[a] Seiichi Inayama,[c] Yoshio Takeuchi,[d] Kenneth L. Kirk[e] and Hitoshi Hori[a,*]

[a]*Department of Biological Science and Technology, Faculty of Engineering, University of Tokushima, Tokushima 770-8506, Japan*
[b]*Medical Research and Development Center, The Tokyo Metropolitan Institute of Medical Science, 3-18-22 Honkomagome, Bunkyo-ku, Tokyo 113-8613, Japan*
[c]*Institute of Oriental Medical Sciences, 2-6-3 Ebisunishi, Shibuya-ku, Tokyo 155-0021, Japan*
[d]*Faculty of Pharmaceutical Sciences, Toyama Medical and Pharmaceutical University, Sugitani 2630, Toyama 930-0194, Japan*
[e]*Laboratory of Bioorganic Chemistry, National Institute of Diabetes and Digestive and Kidney Diseases, National Institute of Health, DHHS, Bethesda, MD 20892, USA*
[f]*Pharmaceutical School of the University of Yanbian, Yanji 133000, China*

Received 14 June 2004; revised 28 June 2004; accepted 28 June 2004
Available online 27 July 2004

Abstract—(*R*)- and (*S*)-Epichlorohydrins were used to prepare the enantiomers of sterically diverse haloacetylcarbamoyl-2-nitroimidazoles that function as hypoxic cell radiosensitizers. The synthetic design allowed for introduction of a side chain of varying bulk that permitted an examination of the steric effects on enantio-discrimination in biological assay systems. The single stereocenter also connected the two pharmacophores—a 2-nitroimidazole moiety critical to hypoxic cell radiosensitization, and a haloacetylcarbamoyl group to function as an anti-angiogenesis pharmacophore. In the chick embryo chorioallantoic membrane (CAM) assay, the *R*-enantiomers possessing the bulky *p-tert*-butylphenyl group showed higher anti-angiogenic activity than the corresponding *S*-enantiomers, while there were no differences in the activity between the enantiomers containing the less bulky methyl and *tert*-butyl groups. Among the compounds we report, *R-p-tert*-butylphenyl-bromoacetylcarbamoyl-2-nitroimidazole, TX-1898, was found to be the most promising candidate for further development of as anti-angiogenic hypoxic cell radiosensitizer.

1. Introduction

Angiogenesis is required for tumor growth and metastasis and, therefore, represents an exciting target for cancer treatment. Angiogenesis is a complex process involving a number of distinct steps, such as endothelial cell migration, proliferation, formation of capillary tubes in endothelial cells, their invasion, and metastasis. These steps are tightly regulated by pro- and anti-angiogenic factors.[1–3] Tumor-related angiogenesis is a multistep process that is initiated through the activity of various pro-angiogenic factors, such as vascular endothelial growth factor (VEGF), basic fibroblast growth factor (bFGF), platelet-derived growth factor (PDGF), insulin-like growth factor (IGF), and interleukin-8 (IL-8). Many enzymes are involved, including such as the matrix metalloproteinases (MMPs), thrombin and methionine aminopeptidase-2 (MetAP-2), urokinase-type plasminogen activator (uPA), and others. Various anti-angiogenic drugs have been developed that target several related growth factor receptors such as VEGF receptors (VEGFR-1 and VEGFR-2), bFGF receptor, and PDGF receptor. Indeed, some of these agents, such as SU5416,[4] ZD6474,[5] SU6668,[6] are now in clinical trials as anti-angiogenic drugs. Our own interest in this area is focused on small molecule anti-angiogenic agents related to the naturally-occurring angiogenic inhibitor fumagillin, and its semi-synthetic analog TNP-470, one of the first substances to be recognized to as having an anti-angiogenic effect.[7–10]

Keywords: Angiogenesis inhibitor; Hypoxic cell radiosensitizer; Haloacetylcarbamoyl-2-nitroimidazole; Enantiomers.
* Corresponding author. Tel.: +81-88-656-7514; fax: +81-88-656-9164; e-mail: hori@bio.tokushima-u.ac.jp

0968-0896/$ - see front matter © 2004 Elsevier Ltd. All rights reserved.
doi:10.1016/j.bmc.2004.06.039

In contrast to anti-angiogenic agents, tumor hypoxia induces the pro-angiogenic genes to stimulate up-regulation of angiogenic and tumor cell survival factors, giving rise to tumor proliferation, radioresistance, angiogenesis, and metastasis.[11] Therefore, hypoxia in solid tumor is one of the targets for the improvement of chemo/radio-therapeutic efficacy. We propose that anti-angiogenic drugs that also function as hypoxic cell radiosensitizers will have synergistic interactions between the hypoxic cytotoxic/hypoxic cell radiosensitizing effect and anti-angiogenic activity leading to destruction of hypoxia-initiated neovasculature.

We have reported the molecular design and synthesis of several 2-nitroimidazole hydroxamate and hydroxamic acid analogs. These include KIN-841,[12] KIN-806,[13] KIN-804,[14,15] and KIN-844,[16] which are bifunctional hypoxic cell radiosensitizers, TX-1877,[17] an anti-metastatic hypoxic cell radiosensitizer, anti-angiogenic hypoxic cytotoxin, TX-402,[18] a protein tyrosine kinase inhibitor TX-1123,[19] and anti-angiogenic/heparin-binding arginine dendrimer TX-1943 and TX-1944[20] (Fig. 1).

We also published previously that the development of racemic bromoacetylcarbamoyl-2-nitroimidazoles such as TX-1845 and TX-1846 as strong radiosensitizers and potent angiogenic inhibitors.[21] The molecular chirality of hypoxic cell radiosensitizers generally has little or no effect on in vitro activity.[22,23] In contrast we have found that there is a significant effect of absolute configuration on anti-angiogenic activity and that a single enantiomer separated from the racemate, often has a higher anti-angiogenic activity than the racemate. For example the *R*-enantiomer of the thienopyridine SR-

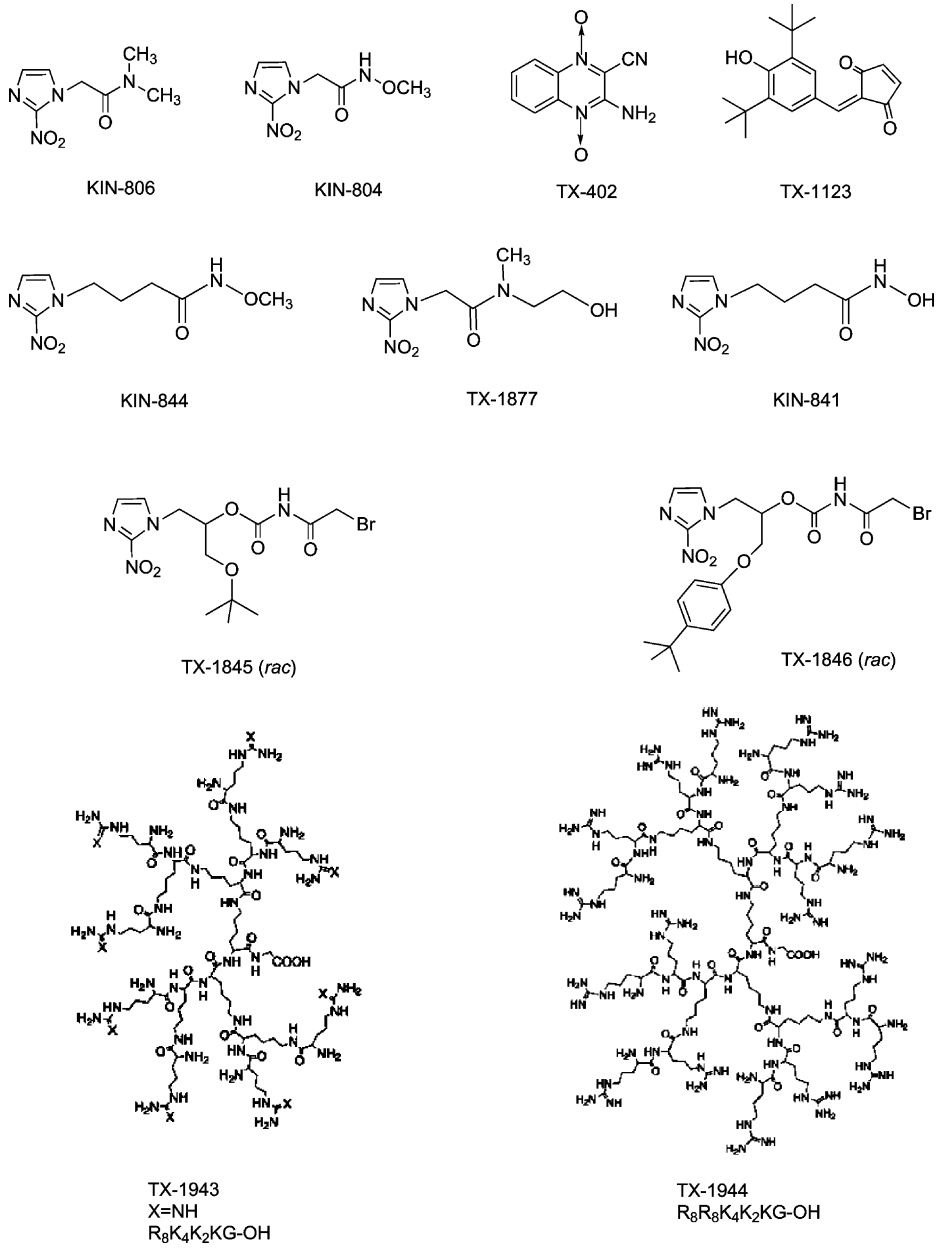

Figure 1. Chemical structures of KIN- and TX-series compounds.

25989 possessed more potent in vitro and in vivo anti-angiogenic properties than the corresponding racemate, and it inhibited metastatic dissemination and growth.[24] Also the *R*,*R*-enantiomer of dihydrobenzofuran lignan showed more potent anti-angiogenic activity than the *S*,*S*-isomer in the chick embryo chorioallantoic membrane (CAM) assay.[25] Molecular shape analysis indicates that there is overlap of target compounds with TNP-470 an anti-angiogenesis drug now in clinical trials, depending on steric bulk and absolute configuration. Based on these considerations, we felt it was important to examine the effects of absolute configuration on a series of haloacetylcarbamoyl-2-nitroimidazole radiosensitizers, compounds that, in racemic form, have shown promising anti-angiogenic and anti-proliferation activity.[21]

In this study we demonstrate the effectiveness of epichlorohydrin as a chiral scaffold wherein the single stereocenter connects a haloacetylcarbamoyl, 2-nitroimidazolyl, and diverse alkyl or aryl groups of varying steric dimensions. We examined the individual enantiomers of haloacetylcarbamoyl-2-nitroimidazoles as protease inhibitors, as anti-angiogenic agents in vitro using a rat lung endothelial (RLE) cell proliferation assay and a chick embryo CAM assay, and also their activities as hypoxic cell radiosensitizers.

2. Results

2.1. Molecular modeling

We carried out geometry and molecular orbital optimizations of the (*R*)-enantiomers of chloroacetylcarbamoyl-2-nitroimidazoles possessing three different alkyl or arylalkyl groups of varying steric bulk–methyl, *tert*-butyl, and *p*-*tert*-butylphenyl. The results were compared to TNP-470 using the B3LYP hybrid density functional theory based the GAUSSIAN 98 programs.[26]

Figure 2 shows their chemical structures, optimized geometries, and the energies of their lowest unoccupied molecular orbitals (LUMOs). The largest region of orbital coefficient distribution in the LUMO of all TX-compounds is localized on the chloroacetylcarbamoyl moiety. With TNP-470, the next LUMO (NLUMO) is localized on this moiety, while the LUMO of this compound is localized on the isoprenyl moiety. Thus, in the TX-compounds, the orbital coefficient distributions of the LUMOs are similar to that of NLUMO of TNP-470. In contrast, the optimized geometries of the TX-compounds were quite similar to that of TNP-470. The relative positions of the chloroacetylcarbamoyl moiety and large alkoxy group of TX-compounds closely approximate the locations of the chloroacetylcarbamoyl and isoprenyl epoxide moieties of TNP-470. In particular, based on orientation of the chloroacetylcarbamoyl group, TX-1897, possessing *p*-*tert*-butylphenyl group, closely resembled the molecular structure of TNP-470. In contrast, after geometry optimizations using the same method, the corresponding (*S*)-enantiomers was not superimposed on the molecular structure of TNP-470. TX-1898 had a molecular structure similar to TX-1897, but possessing lower E_{LUMO} value (($E_{LUMO} = -0.05804$ hartree (-1.57869 eV)) than that of TX-1897 ($E_{LUMO} = -0.04915$ hartree (-1.33688 eV)) as shown in Figures 3 and 2.

2.2. Synthesis

As shown in Scheme 1, (*R*)- and (*S*)-*tert*-butyl glycidyl ether [(***R***)- and (***S***)-**1**], and (*R*)- and (*S*)-*p*-*tert*-butylphenyl glycidyl ether [(***R***)- and (***S***)-**2**] were prepared from the corresponding (*S*)- and (*R*)-epichlorohydrins (99.9% pure, 98.9% ee; 99.6% pure, 98.6% ee, respectively) by reaction with *tert*-butanol using a catalytic amount of borontrifluoride ether complex, and *p*-*tert*-butylphenol in aqueous sodium hydroxide, respectively. The yields ranged from 54% to 90%.

Following the procedure we used for the preparation the methyl derivatives [(***R***)- and (***S***)-**3**], the enantiomers of 2-hydroxy-3-(2-nitro-1*H*-imidazolyl)-propyl ethers [(***R***)- and (***S***)-**4, 5**], were prepared by reaction of the

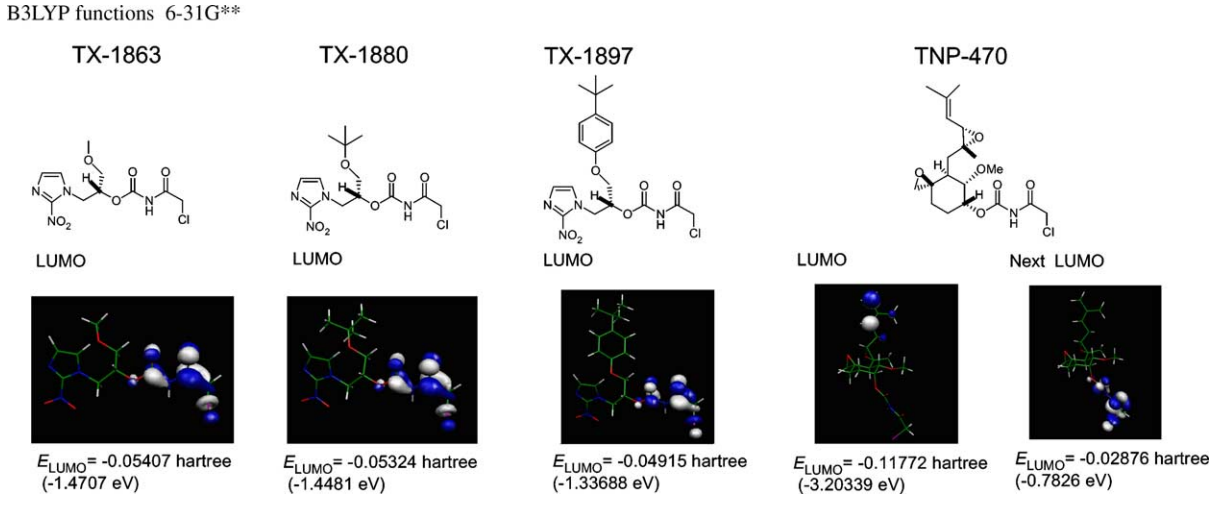

Figure 2. LUMO of the geometrically optimized (*R*)-chloroacetylcarbamoyl-2-nitroimidazoles with the B3LYP hybrid density functional in conjunction with the 6-31G(d) basis set using the GAUSSIAN 98 suite of program.

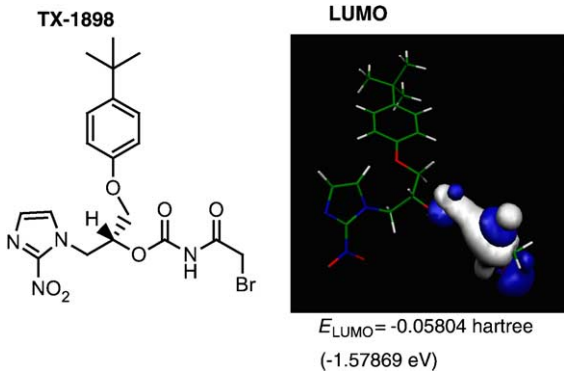

Figure 3. LUMO of the geometrically optimized (*R*)-bromoacetylcarbamoyl-2-nitroimidazoles with the B3LYP hybrid density functional in conjunction with the 6-31G(d) basis set using the GAUSSIAN 98 suite of program.

enantiomerically pure glycidyl ethers [(***R***)- and (***S***)**-1, 2**], with 2-nitroimidazole in the presence of ethanolic sodium carbonate. Treatment of the enantiomerically pure propanols [(***R***)- and (***S***)**-3, 4, 5**] with highly purified chloro- or bromo-acetyl isocyanates for 30 min in CH_2Cl_2 gave the chiral haloacetylcarbamoyl-2-nitroimidazoles derivatives in good yield (72–98%) as shown in Scheme 2.

The structures and yields of the single enantiomers of haloacetylcarbamoyl-2-nitroimidazoles are shown in Table 1. The methyl derivatives (TX-1863, TX-1878, TX-1866, and TX-1879) were re-synthesized following the procedure described in our previous paper.[27]

2.3. Biological activity

2.3.1. Serine protease inhibitory activity.[28] Serine proteases, such as thrombin[29] and urokinase-type plasminogen activator (uPA),[30] and metalloproteases MMPs participate in tumor growth and angiogenesis, and several tyrosine kinases, such as VEGF, PDGF, and Met

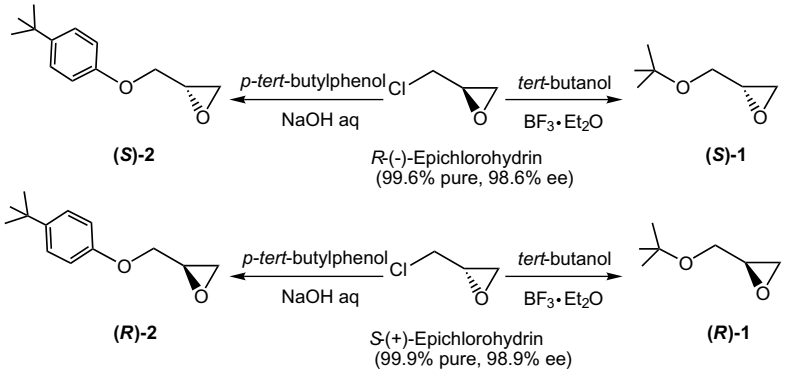

Scheme 1. Synthesis of single enantiomeric alkyl (aryl) glycidyl ethers.

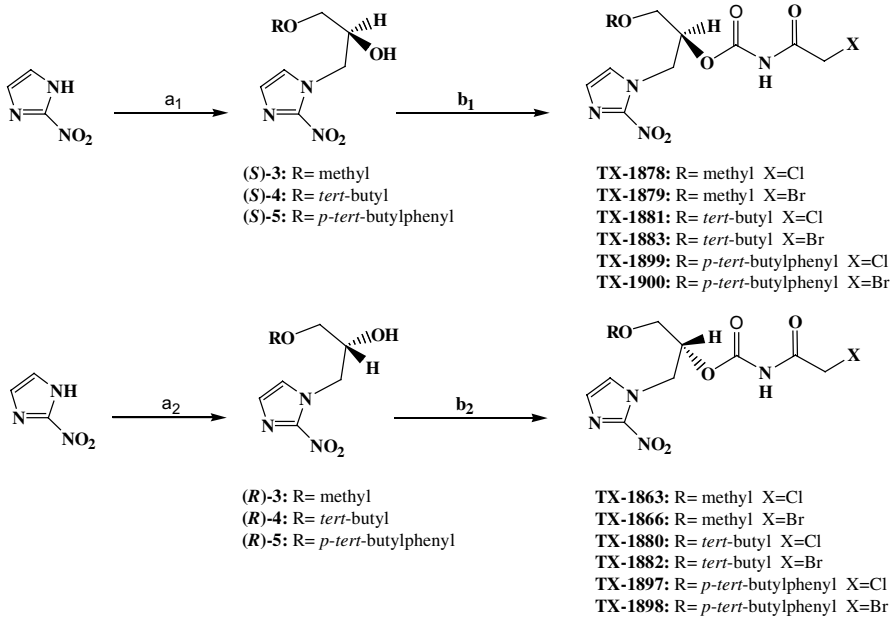

Scheme 2. Synthesis of single enantiomer of haloacetylcarbamoyl-2-nitroimidazoles; (a_1): (*S*)-alkyl glycidyl ether/anhydrous EtOH, Na_2CO_3, reflux; (b_1): haloacetylisocyanate/anhydrous CH_2Cl_2, rt; (a_2): (*R*)-alkyl glycidyl ether/anhydrous EtOH, Na_2CO_3, reflux; (b_2): haloacetylisocyanate/anhydrous CH_2Cl_2, rt.

Table 1. Enantiomeric haloacetylcarbamoyl-2-nitroimidazole radiosensitizers

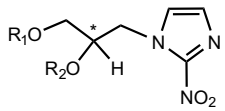

Radiosensitizer	Configuration	R_1	R_2	Yield (%)
TX-1863	*R*	Methyl	$CONHCOCH_2Cl$	96
TX-1878	*S*	Methyl	$CONHCOCH_2Cl$	90
TX-1866	*R*	Methyl	$CONHCOCH_2Br$	98
TX-1879	*S*	Methyl	$CONHCOCH_2Br$	96
TX-1880	*R*	*t*-Butyl	$CONHCOCH_2Cl$	73
TX-1881	*S*	*t*-Butyl	$CONHCOCH_2Cl$	72
TX-1882	*R*	*t*-Butyl	$CONHCOCH_2Br$	77
TX-1883	*S*	*t*-Butyl	$CONHCOCH_2Br$	74
TX-1897	*R*	*p*-*t*-Butylphenyl	$CONHCOCH_2Cl$	95
TX-1899	*S*	*p*-*t*-Butylphenyl	$CONHCOCH_2Cl$	91
TX-1898	*R*	*p*-*t*-Butylphenyl	$CONHCOCH_2Br$	98
TX-1900	*S*	*p*-*t*-Butylphenyl	$CONHCOCH_2Br$	93

tyrosine kinase[31] are also involved in tumor angiogenesis. Therefore, we examined the inhibitory activities of the individual single enantiomers of haloacetylcarbamoyl-2-nitroimidazoles as inhibitors of serine proteases, porcine pancreatic (PP) elastase. As shown in Table 2, compounds containing the more bulky *p*-*tert*-butylphenyl group were more active than those possessing the corresponding *tert*-butyl and methyl groups. Regarding the haloacetyl group, bromoacetyl derivatives showed more active than the corresponding chloroacetyl derivatives, as described previously.[21] It is noteworthy that the *R*-isomers were more active than the corresponding *S*-isomers. Compound TX-1898, which has the bulky *p*-*tert*-butylphenyl group, the bromoacetyl group, and the 2-nitroimidazole moiety appended to the *R*-stereocenter was the most potent PP elastase inhibitor among the compounds tested here.

2.3.2. RLE cell proliferation inhibitory activity.[32] The potencies of inhibition of proliferation of RLE cells in vitro are shown in Table 3. The rank order of activity (IC_{50} values) of the compounds tested was: TX-1897 (7.5 μM) > TX-1880 (71 μM) > TX-1863 (325 μM), TX-1899 (6.5 μM) > TX-1881 (80 μM) > TX-1878 (275 μM), TX-1898 (1.4 μM) > TX-1882 (6.3 μM) > TX-1866 (20 μM), TX-1900 (0.9 μM) > TX-1883 (6.9 μM) > TX-1879 (17 μM). The *p*-*tert*-butylphenyl bromoacetylcarbamoyl derivatives, TX-1900 and TX-1898, showed the most potent activity.

Table 2. Inhibition of single enantiomeric haloacetylcarbamoyl-2-nitroimidazole radiosensitizers on porcine pancreatic elastase

Ether moiety	Halogen	TX-No	K_i (μM)[a]	
			R-Isomer	*S*-Isomer
Me	Cl	TX-1863	1180	
		TX-1878		1750
Me	Br	TX-1866	66	
		TX-1879		220
t-Bu	Cl	TX-1880	260	
		TX-1881		557
t-Bu	Br	TX-1882	42	
		TX-1883		55
p-*t*-BuPh	Cl	TX-1897	30	
		TX-1899		56
p-*t*-BuPh	Br	TX-1898	9	
		TX-1900		14

[a] Substrate: succinyl-Ala-Ala-Ala-*p*NA.

Table 3. Inhibition of single enantiomeric haloacetylcarbamoyl-2-nitroimidazole radiosensitizers on RLE cell proliferation

Ether moiety	Halogen	TX-No	IC_{50} (μM)	
			R-Isomer	*S*-Isomer
Me	Cl	TX-1863	325	
		TX-1878		275
Me	Br	TX-1866	20	
		TX-1879		17
t-Bu	Cl	TX-1880	71	
		TX-1881		80
t-Bu	Br	TX-1882	6.3	
		TX-1883		6.9
p-*t*-BuPh	Cl	TX-1897	7.5	
		TX-1899		6.5
p-*t*-BuPh	Br	TX-1898	1.4	
		TX-1900		0.9

There was no significant difference between the activities of the individual enantiomers. The potency of inhibition increased with the increasing size of the ether moiety (methyl < *tert*-butyl < *p*-*tert*-butylphenyl). The bromoacetylcarbamoyl derivatives were about 5–10 times more effective than the corresponding chloroacetylcarbamoyl derivatives.

2.3.3. Anti-angiogenic activity.[33] Anti-angiogenic activities of the compounds that were measured using the chick embryo CAM assay are shown in Table 4. All compounds tested showed high angiogenic inhibitory activity. In particular, the *p*-*tert*-butylphenyl-bromoacetylcarbamoyl derivatives, TX-1898 and TX-1900, inhibited angiogenesis by more than 80% at their lowest dose of 5 μg/pellet. Both enantiomers of all haloacetylcarbamoyl-2-nitroimidazoles examined exhibited potent than TNP-470. In compounds possessing the

Table 4. Antiangiogenic activity of enantiomeric haloacetylcarbamoyl-2-nitroimidazoles in CAM assay

Ether moiety	Halogen	TX-No	μg/pellet	Inhibition (%)	
				R-Isomer	*S*-Isomer
Me	Cl	TX-1863	100	80	
		TX-1878	100		83
Me	Br	TX-1866	100	100	
		TX-1879	100		100
t-Bu	Cl	TX-1880	10	55	
		TX-1881	10		53
t-Bu	Br	TX-1882	10	61	
		TX-1883	10		77
p-*t*-BuPh	Cl	TX-1897	10	64	
		TX-1899	10		58
p-*t*-BuPh	Br	TX-1898	5	93	
		TX-1900	5		82
		TNP-470	10	81.8	
			5	78.1	

Table 5. Radiosensitizing effects and log *P* of enantiomeric haloacetylcarbamoyl-2-nitroimidazole radiosensitizers on EMT6/KU cells

Radiosensitizer	log *P*[a]	ER (10 μM)	
	calcd/obsd	*R*-Isomer	*S*-Isomer
TX-1880	1.45/1.14	1.76	
TX-1881	1.45/1.13		1.75
TX-1882	1.57/1.22	1.82	
TX-1883	1.57/1.21		1.83
TX-1897	3.68/3.16	1.73 (1 μM)[b]	
TX-1899	3.68/3.31		1.90
			1.75 (1 μM)
TX-1898	3.79/2.90	1.80	
TX-1900	3.79/3.25		1.74

[a] log *P* are calculated by Pallas 3.0 and measured in *n*-octanol-phosphate buffer (pH = 7.4).
[b] Measured at 1 μM because of cytotoxicity at 10 μM without irradiation.

bulky *p*-*tert*-butylphenyl ether moiety, the *R*-isomers were more anti-angiogenic than the corresponding *S*-isomers. Thus the potencies can be ranked as follows: TX-1898 (93% at 5 μg/pellet) > TX-1900 (82% at 5 μg/pellet), TX-1897 (64% at 10 μg/pellet) > TX-1899 (58% at 10 μg/pellet). This trend was more significant for bromoacetyl derivatives than chloroacetyl derivatives. There was no difference in the anti-angiogenic activities of the single enantiomers of the haloacetylcarbamoyl-2-nitroimidazole radiosensitizers containing the less sterically bulky methyl and *tert*-butyl ethers. The rank order of potency is: TX-1863 (80% at 100 μg/pellet) and TX-1878 (83% at 100 μg/pellet) or TX-1866 (100% at 100 μg/pellet) and TX-1879 (100% at 100 μg/pellet). From this it can be seen that the bulky *p*-*tert*-butylphenyl group increases the anti-angiogenic activity of the haloacetylcarbamoyl-2-nitroimidazoles in the chick embryo CAM assay, but this positive, albeit modest, steric effect is seen only with the *R*-enantiomer. In contrast there was no difference in potencies of the enantiomers of the compounds possessing the less bulky methyl and *tert*-butyl ethers. As expected, the bromoacetyl derivatives were more potent than the corresponding chloroacetyl derivatives: the rank order of potency was TX-1898 (*R*) > TX-1897 (*R*), TX-1900 (*S*) > TX-1899 (*S*).

2.3.4. In vitro radiosensitizing activity.[34] In vitro radiosensitizing activities of the compounds tested are shown in Table 5. All compounds exhibited strong hypoxic cell radiosensitizing activities at concentrations of 10 μM. Consistent with the results contained in our previous report, there were no differences of radiosensitizing activity between stereoisomers.[21] The radiosensitizing enhancement ratio (ER) values of the compounds in this study also showed a positive correlation with their partition coefficient log *P*.

3. Discussion

As part of our research to develop effective cancer chemotherapeutic agents, we have developed compounds that combine radiosensitizing activity with anti-angiogenic activity. In our previous report,[21] we found the racemic haloacetylcarbamoyl-2-nitroimidazole hypoxic cell radiosensitizers, such as KIN-1800, TX-1835, TX-1836, TX-1844, TX-1845, and TX-1846, were also potent angiogenesis inhibitors activity that we ascribe to the presence of the reactive haloacetylcarbamoyl group. To examine the structure–activity relationship of a series of single enantiomeric anti-angiogenic haloacetylcarbamoyl-2-nitroimidazole hypoxic cell radiosensitizers we exploited the functionality and stereocenter of epichlorohydrin to prepare individual enantiomers of haloacetylcarbamoyl-2-nitroimidazoles. These were adorned with groups of increasing bulk (methyl, *tert*-butyl, *p*-*tert*-butylphenyl) through an ether linkage. This allows the study of effects of lipophilicity and steric factors in the interactions with angiogenesis-related enzymes, particularly as a function of absolute stereochemistry.

Recently MetAP-2 has been identified as one of the molecular targets of the anti-angiogenic agent TNP-470 and its 'parent' fumagillin. Sin et al.[35] have shown that fumagillin selectively inhibits the *S. cerevisiae* MetAP-2 protein in vivo, and Griffith et al.[36,37] revealed that TNP-470 covalently binds to MetAP-2 through reaction of His 231 with the ring epoxide of TNP-470. From these results they suggested that MetAP-2 may play a critical role in the proliferation of endothelial cells and thus could represent a promising target for the development of new anti-angiogenic drugs. However, Griffith et al. did not discuss a possible role of the chloroacetylcarbamoyl group of TNP-470 in its anti-angiogenic activity.[36,37] From the X-ray data of the fumagillin or TNP-470 complex with MetAP-2, the four different substituents on cyclohexane ring are shown to be arranged asymmetrically to fit neatly into the binding pocket of MetAP-2.[38,39] In this arrangement the cyclohexane ring functions as a tetravalent chiral scaffold. Our molecular modeling data for the compounds in our present study show that if the bulky *p*-*tert*-butylphenyl were present, a single stereocenter could function as chiral scaffold to produce a similar structural array. Thus, the optimized geometry of molecular structure of TX-1897 possessing the *R*-stereocenter closely resembles the optimized geometry of the molecular structure of TNP-470 (Fig. 4).

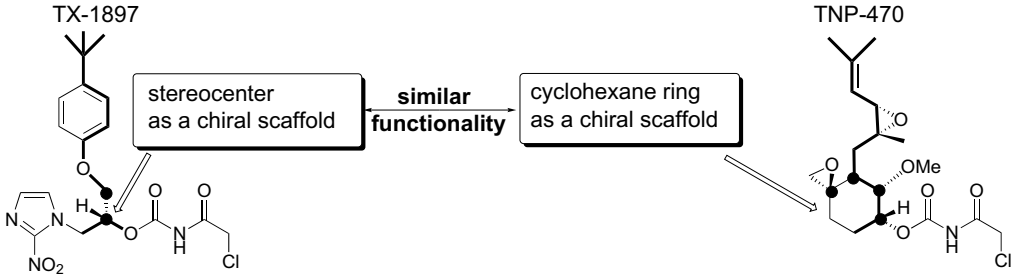

Figure 4. The molecular similarity of TX-1897 and TNP-470. The similar stereocenter of TX-1897 acts as a chiral scaffold in a similar manner as the four-chiral stereocenter-cyclohexane ring chiral scafforld of TNP-470. The symbol (•) indicates the carbon atoms constituting the scaffold.

In contrast, the compounds with the less bulky methyl (TX-1863) or *tert*-butyl (TX-1880) groups showed no similarity with the optimized molecular structure of TNP-470 (Fig. 2). Differing only in the nature of the halogen, TX-1898 also may be expected to have a molecular structure similar to TNP-470, in analogy with TX-1897. Based on these considerations, we reasoned that TX-1897 and TX-1898 might be potent inhibitors of MetAP-2, the molecular target of angiogenesis inhibitor TNP-470. The corresponding *S*-enantiomers, TX-1899 and TX-1900, cannot be superimposed on the optimized molecular structure of TNP-470 and thus would be expected to have lower anti-angiogenic activity in the CAM assay. We note that a chiral scaffold usually refers to a platform with multiple functionality and two or more chiral centers with fixed geometry, example of which include such structures as indolizidine alkaloids[40] and sugars.[41] We consider that in chiral haloacetylcarbamoyl-2-nitroimidazoles, even the single stereocenter functioned as a chiral scaffold for their biological activities including anti-angiogenic activity.

The results of biological evaluation showed that the effect of stereochemistry varied with the system being studied. In the PP elastase inhibitory assay the *R*-isomers were more active than the corresponding *S*-isomers. In particular, TX-1898 and TX-1897 possessing the bulky *p*-*tert*-butylphenyl group showed impressive activity. In the CAM assay the *R*-isomers were slightly more active than the *S*-isomers. All *p*-*tert*-butylphenyl-haloacetylcarbamoyl-2-nitroimidazole compounds, TX-1898, TX-1900, TX-1897 and TX-1899, were more potent in the chick embryo CAM assay than the haloacetylcarbamoyl-containing fumagillin synthetic analog, TNP-470 (Table 4). This high activity, in combination with their potent radiosensitizing activity, makes them particularly promising as candidates for development as bifunctional chemotherapeutic agents.

In interactions of our compounds with enzymes or receptors involved with angiogenesis, the presence of the bulky *p*-*tert*-butylphenyl group apparently is required before significant stereo-differentiation is observed. The preference for the *R*-isomer is seen most clearly in inhibition of PP elastase. Other targets can be considered. For example, Keezer et al.[42] have recently reported that TNP-470 targeted the endothelial cell cytoskeleton through altered regulation of heat shock protein 27 (Hsp 27) and cofilin. We plan to evaluate the effects of our compounds on these proteins.

The haloacetyl functionality appears to be critical to activity, as we have previously suggested.[21] In this regard, Kim et al.[43] recently reported that in calf pulmonary artery endothelial cells, TNP-470 showed at least 10,000 times higher anti-proliferation activity than did fumagillol (deschloroacetylcarbamoyl TNP-470). The effect of chloroacetylcarbamoyl group was more pronounced in fumagillol derivatives with the methoxy group at its 5-position. From these results, we consider that in TNP-470, the four functional groups at 3, 4, 5, and 6-position of stereo-scaffold cyclohexane ring oriented the molecular geometry to maximize interactions with angiogenesis-related enzymes such as MetAP-2. Kim's results support our previous conclusion that the haloacetylcarbamoyl group makes an important contribution as an anti-angiogenic pharmacophore.[21] In addition, Satchi-Fainaro et al.[44] recently reported the synthesis of the *N*-(2-hydroxypropyl)methacrylamide (HPMA) copolymer-TNP-470 as an anti-angiogenic agent shown in Figure 5. The synthesis involved conjugation of TNP-470 to HPMA copolymer-Gly-Phe-Leu-Gly-ethylenediamine by displacement of the terminal chlorine of TNP-470. This indicates that in TNP-470, the chloroacetylcarbamoyl group is more reactive than the epoxide on the cyclohexane ring, for general nucleophilic substitution reaction. However, the copolymer showed potent activity, but now not possessing a chloroacetyl group. In addition, that interaction of an electrophile with an enzyme nucleophile is more influenced by proper orientation at the active site that the relative reactivities. We feel these results support our previous suggestion, that the haloacetylcarbamoyl group

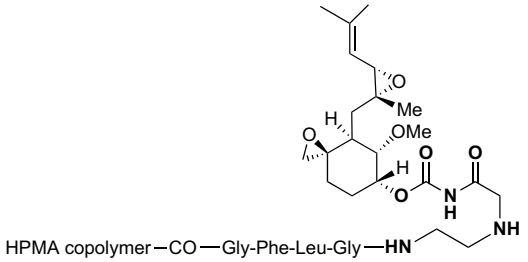

Figure 5. The structure of HPMA copolymer-TNP-470 (modified Fig. 1 in Ref. 44).

represents an important pharmacophore and can play an important part in angiogenesis-related biotransformation.

In summary, we have carried out syntheses of the individual enantiomers of haloacetylcarbamoyl-2-nitroimidazole as anti-angiogenic hypoxic cell radiosensitizers. The synthetic design allows introduction of diversity in the side-chain ether function, as illustrated by the introduction of methyl, *tert*-butyl, *p*-*tert*-butylphenyl in this series. The data from biological evaluation suggest that the (*R*)-*p*-*tert*-butylphenyl-bromoacetylcarbamoyl-2-nitroimidazole hypoxic cell radiosensitizer, TX-1898, may be a very promising candidate for further development as an anti-angiogenic hypoxic cell radiosensitizer.

4. Experimental

4.1. General procedures

^{1}H NMR spectra were recorded on a JEOL JNM-EX400 spectrometer (400 MHz) with tetramethylsilane as the internal standard. Chemical shifts were reported in ppm. Coupling constants were reported in Hz. IR spectra were reported in KBr pellet on a Perkin–Elmer 1600 spectrometer. High-resolution mass spectra (HRMS) were measured on a JEOL JMS-SX102A mass spectrometer using a fast atom bombardment (FAB) and EI. Reaction was monitored by analytical thin-layer chromatograpy (TLC) with use of Merck silica gel $60F_{254}$ glass plates and Merck aluminum oxide $60F_{254}$ neutral (Type E). Column chromatography was performed on Merck silica gel 60 (230–400 mesh). Optical rotations were determined on JASCO DIP-370 digital polarimeter. All melting points were determined with a micromelting point measurement apparatus (MP-j 3 model) and were uncorrected. Elemental analysis was performed with a Yanako CHN Corder MT-5. All the chemicals were purchased from Wako Pure Chemical Industries, Ltd (Osaka, Japan). (*S*)-(+)-epichlorohydrin (99.9% pure, 98.9% ee) and (*R*)-(−)-epichlorohydrin (99.6% pure, 98.6% ee) was provided from DAISO Co., Ltd (Osaka, Japan).

4.2. Molecular modeling methods

The molecular geometries and molecular calculations were performed with the B3LYP hybrid density functional in conjunction with the 6-31G** basis set using the GAUSSIAN 98 suite of programs.[26]

4.3. General procedure for synthesis of (*R*)-or (*S*)-*tert*-butyl glycidyl ether [(*R*/*S*)-1]

To a solution of *tert*-butanol (37.1 g, 500 mmol) and boron trifluoride ether complex (46–49%) (88.7 mg, 0.625 mmol) in anhydrous CH_2Cl_2 (100 mL), (*S*)-or (*R*)-epichlorohydrin (11.6 g, 125 mmol) was added. After being stirred until no starting material remained, the reaction mixture was evaporated in vacuo. Sodium hydroxide solution (7 mL, 20%) was added to the residue. The resulting mixture was stirred at room temperature for 17 h, and the organic layer was washed with water and separated. The aqueous layer was extracted with ethyl ether, the organic fraction was dried with anhydrous sodium sulfate and evaporated in vacuo to give a colorless liquid.

4.3.1. (*R*)-*tert*-Butyl glycidyl ether ((*R*)-1). (14.7 g, 90%), $[\alpha]_D^{28}$ +3.81 (*c* 1.4, $CHCl_3$); ^{1}H NMR ($CDCl_3$) δ 1.21 (s, 9H), 2.63 and 2.81 (m, each 1H), 3.11 (m, 1H), 3.43 and 3.53 (m, each 1H). IR (cm^{-1}): 2976, 1472, 1365, 1252, 1236, 1197, 1090, 1023, 908, 875, 843. Anal. Calcd for $C_7H_{14}O_2$: C, 64.58; H, 10.84. Found: C, 64.48; H, 10.96.

4.3.2. (*S*)-*tert*-Butyl glycidyl ether ((*S*)-1). (13.7 g, 84%), $[\alpha]_D^{28}$ −3.84 (*c* 1.2, $CHCl_3$); ^{1}H NMR ($CDCl_3$) δ 1.21 (s, 9H), 2.63 and 2.81 (m, each 1H), 3.11 (m, 1H), 3.42 and 3.53 (m, each 1H). IR (cm^{-1}): 2974, 1473, 1365, 1253, 1194, 1087, 1022, 973, 874, 747. Anal. Calcd for $C_7H_{14}O_2$: C, 64.58; H, 10.84. Found: C, 64.42; H, 10.66.

4.4. General procedure for the synthesis of (*R*)-or (*S*)-*p*-*tert*-butylphenyl glycidyl ether [(*R*/*S*)-2]

To (*R*)-or (*S*)-epichlorohydrin (9.25 g, 100 mmol) heated to 64 °C was added to a solution of *p*-*tert*-butylphenol (7.51 g, 50 mmol) and sodium hydroxide (2.1 g, 52.5 mmol, in 16 mL H_2O) over 8 h, with vigorous stirring. The crude product that separated from the aqueous layer and washed with H_2O, and the water layer was extracted with ethyl ether. The organic layer was washed with NaCl (satd) aq, dried with anhydrous sodium sulfate, and evaporated in vacuo. The residue was purified by silica gel column chromatography with hexane and acetyl acetate, to give the product as a colorless liquid.

4.4.1. (*S*)-*p*-*tert*-Butylphenyl glycidyl ether ((*S*)-2). (5.54 g, 54%), $[\alpha]_D^{28}$ +1.53 (*c* 1.2, $CHCl_3$); ^{1}H NMR ($CDCl_3$) δ 1.30 (s, 9H), 2.73 and 2.88 (each m, each 1H), 3.33 (m, 1H), 3.95 and 4.17 (m, each 1H), 6.84 and 7.29 (dd, J = 5.5, 5.9 Hz, each 2H). IR (cm^{-1}): 2962, 1609, 1514, 1457, 1364, 1247, 1186, 1037, 917, 829. Anal. Calcd for $C_{13}H_{18}O_2$: C, 75.69; H, 8.80. Found: C, 75.41; H, 8.67.

4.4.2. (*R*)-*p*-*tert*-Butylphenyl glycidyl ether ((*R*)-2). (1.57 g, 51%), $[\alpha]_D^{28}$ −0.95 (*c* 1.2, $CHCl_3$); ^{1}H NMR ($CDCl_3$) δ 1.30 (s, 9H), 2.74 and 2.89 (each m, each 1H), 3.35 (m, 1H), 3.93 and 4.15 (m, each 1H), 6.84 and 7.29 (dd, J = 5.5, 5.9 Hz, each 2H). IR (cm^{-1}): 2953, 1610, 1512, 1461, 1364, 1292, 1256, 1184, 1117, 1041, 825. Anal. Calcd for $C_{13}H_{18}O_2$: C, 75.69; H, 8.80. Found: C, 75.85; H, 8.99.

4.5. General procedure for synthesis of (*R*)- or (*S*)-alkoxy-1-(2-nitroimidazolyl)-2-propanols

To a suspension of 2-nitroimidazole (1.69 g, 15 mmol) and sodium carbonate (853 mg, 8 mmol) in anhydrous EtOH (50 mL) was added *R*- or *S*-alkyl glycidyl ether (31 mmol). After being refluxed for 6 h, the reaction mixture was filtered and washed with CH_2Cl_2. The filtrate

was evaporated in vacuo to give a semi-solid residue, which was purified by column chromatography on silica gel with CH_2Cl_2 and MeOH to afford (*R*)- or (*S*)-alkoxy-1-(2-nitroimidazolyl)-2-propanols (TX-1888, TX-1860, TX-1894, TX-1893, TX-1896, and TX-1895).

4.5.1. TX-1888((*S*)-3). Yield, 82% as yellow semi-solid, $[\alpha]_D^{28}$ +5.79 (*c* 0.3, CH_3OH); ^1H NMR ($CDCl_3$) δ 3.30 (s, 3H), 3.44 and 3.51 (m, 2H), 4.16 (m, 1H), 4.37 and 4.71 (m, 2H), 7.05 and 7.22 (s, 2H). IR (cm^{-1}): 3425, 2932, 1541, 1490, 1362, 1280, 1124, 838. Anal. Calcd for $C_7H_{11}N_3O_4$: C, 41.79; H, 5.51; N, 20.89. Found: C, 42.05; H, 5.47; N, 21.08.

4.5.2. TX-1860 ((*R*)-3). Yield, 81% as yellow semi-solid, $[\alpha]_D^{28}$ −8.86 (*c* 0.3, CH_3OH), ^1H NMR ($CDCl_3$) δ 3.30 (s, 3H), 3.40 and 3.53 (m, 2H), 4.16 (m, 1H), 4.42 and 4.67 (m, 2H), 7.15 and 7.26 (s, 2H). IR (cm^{-1}): 3425, 2935, 1541, 1491, 1362, 1283, 1122, 838. Anal. Calcd for $C_7H_{11}N_3O_4$: C, 41.79; H, 5.51; N, 20.89. Found: C, 42.00; H, 5.36; N, 21.84.

4.5.3. TX-1894 ((*S*)-4). Yield, 85% as a yellow solid, mp 95–96 °C; $[\alpha]_D^{28}$ +3.55 (*c* 0.5, $CHCl_3$);^1H NMR ($CDCl_3$) δ 1.19 (s, 9H), 3.35 and 3.53 (dd, *J* = 5.2, 4.0 Hz, each 1H), 4.07 (m, 1H), 4.45 and 4.62 (dd, *J* = 7.4, 3.6 Hz, each 1H), 7.14 and 7.21 (d, *J* = 1.6, 0.8 Hz, each 1H). IR (cm^{-1}): 3384, 2974, 2863, 1534, 1490, 1362, 1287, 1196, 1157, 1063, 964, 836, 792. Anal. Calcd for $C_{10}H_{17}N_3O_4$: C, 49.37; H, 7.04; N, 17.27. Found: C, 49.58; H, 6.84; N, 17.06.

4.5.4. TX-1893 ((*R*)-4). Yield, 72% as a yellow solid, mp 95–96 °C; $[\alpha]_D^{28}$ −2.32 (*c* 0.5, $CHCl_3$); ^1H NMR ($CDCl_3$) δ 1.19 (s, 9H), 3.35 and 3.53 (dd, *J* = 5.0, 4.0 Hz, each 1H), 4.07 (m, 1H), 4.46 and 4.62 (dd, *J* = 3.2, 3.6 Hz, each 1H), 7.14 and 7.21 (d, *J* = 1.2 Hz, each 1H). IR (cm^{-1}): 3405, 2974, 2872, 1579, 1492, 1364, 1272, 1195, 1159, 1097, 1061, 1015, 836, 790, 743, 692. Anal. Calcd for $C_{10}H_{17}N_3O_4$: C, 49.37; H, 7.04; N, 17.27. Found: C, 49.37; H, 6.78; N, 17.05.

4.5.5. TX-1896 ((*S*)-5). Yield, 73% as a yellow solid, mp 183–184 °C; $[\alpha]_D^{28}$ −9.28 (*c* 0.2, $CHCl_3$); ^1H NMR ($CDCl_3$) δ 1.29 (s, 9H), 3.97 and 4.09 (dd, *J* = 5.2, 5.6 Hz, each 1H), 4.39 (m, 1H,), 4.55 and 4.81 (dd, *J* = 7.6, 3.6 Hz, each 1H), 6.84 and 7.32 (dd, *J* = 2.4 Hz, each 2H), 7.15 and 7.22 (dd, *J* = 0.8 Hz, each 1H). IR (cm^{-1}): 3374, 3128, 2964, 2871, 1579, 1512, 1492, 1364, 1189, 1107, 1025, 825. Anal. Calcd for $C_{10}H_{17}N_3O_4$: C, 60.17; H, 6.63; N, 13.16. Found: C, 59.91; H, 6.45; N, 12.97.

4.5.6. TX-1895 ((*R*)-5). Yield, 71% as a yellow solid, mp 183–184 °C; $[\alpha]_D^{28}$ +8.30 (*c* 0.2, $CHCl_3$); ^1H NMR ($CDCl_3$) δ 1.30 (s, 9H), 3.97 and 4.11 (dd, *J* = 5.4, 4.2 Hz, each 1H), 4.38 (m, 1H), 4.56 and 4.81 (dd, *J* = 6.9, 3.4 Hz, each 1H), 6.84 and 7.32 (dd, *J* = 1.4, 1.8 Hz, each 2H), 7.16 and 7.22 (dd, *J* = 1.2 Hz, each 1H). IR (cm^{-1}): 3384, 3128, 2964, 2871, 1579, 1512, 1492, 1364, 1246, 1189, 1117, 1082, 1056, 1025, 825. Anal. Calcd for $C_{10}H_{17}N_3O_4$: C, 60.17; H, 6.63; N, 13.16. Found: C, 59.90; H, 6.50; N, 12.87.

4.6. General procedure for synthesis of (2*R*)- or (2*S*)-haloacetylcarbamoyl-2-nitroimidazoles

To a solution of (*R*)- or (*S*)-3-substituted-1-(2-nitroimidazolyl)-2-propanols (TX-1894, TX-1893, TX-1895 or TX-1896, 2.1 mmol) in anhydrous CH_2Cl_2 (10 mL), was added haloacetyl isocyanate (either chloroacetyl isocyanate or bromoacetyl isocyanate) (4.2 mmol), prepared immediately before use. After being refluxed for 30 min, the reaction mixture was filtered and the filtrate was washed with CH_2Cl_2. The residue remaining after evaporation in vacuo was purified by silica gel column chromatography with CH_2Cl_2 and AcOEt, to give (2*R*)- or (2*S*)-haloacetylcarbamoyl-2-nitroimidazoles (TX-1863, TX-1878, TX-1866, TX-1879, TX-1880, TX-1881, TX-1882, TX-1883, TX-1897, TX-1898, TX-1899, TX-1900).

4.6.1. TX-1863. Yield, 96% as a yellow solid, mp 100–101 °C; $[\alpha]_D^{28}$ +27.9 (*c* 0.3, CH_3OH); ^1H NMR ($CDCl_3$) δ 3.40 (s, 3 H), 3.62(m, 2H), 4.36(d, *J* = 15.4 Hz, 2H), 4.59 and 4.92 (dd, *J* = 14.4 Hz, 2H), 5.32 (m, 1H), 7.14 and 7.28 (s, 2H). IR (cm^{-1}): 3424, 1791, 1718, 1541, 1490, 1363, 1267, 1102, 839, 771, 632. HRMS (FAB) *m*/*z* (MH^+): calcd for $C_{10}H_{13}ClN_4O_6$, 321.0573; found, 321.0601.

4.6.2. TX-1878. Yield, 90% as a yellow solid, mp 101–102 °C; $[\alpha]_D^{28}$ −30.3 (*c* 0.3, CH_3OH); ^1H NMR ($CDCl_3$) 3.42 (s, 3 H), 3.62(m, 2H), 4.36(d, *J* = 15.4 Hz, 2H), 4.58 and 4.92 (dd, *J* = 14.4 Hz, 2H), 5.32 (m, 1H), 7.14 and 7.28 (s, 2H). IR (cm^{-1}): 3425, 1789, 1717, 1541, 1490, 1364, 1210, 1103, 839, 768, 653. HRMS (FAB) *m*/*z* (MH^+): calcd for $C_{10}H_{13}ClN_4O_6$, 321.0573; found, 321.0596.

4.6.3. TX-1866. Yield, 98% as a yellow solid, mp 108–109 °C; $[\alpha]_D^{28}$ +39.9 (*c* 0.3, CH_3OH); ^1H NMR ($CDCl_3$) δ 3.42 (s, 3 H), 3.62(m, 2H), 4.13(d, *J* = 12.8 Hz, 2H), 4.59 and 4.92 (dd, *J* = 14.4, 14.8 Hz, 2H), 5.33 (m, 1H), 7.14 and 7.28 (s, 2H). IR (cm^{-1}): 3388, 1786, 1717, 1541, 1490, 1364, 1221, 1100, 839, 768, 599. HRMS (FAB) *m*/*z* (MH^+): calcd for $C_{10}H_{13}BrN_4O_6$, 365.0079; found, 365.0092.

4.6.4. TX-1879. Yield, 96% as a yellow solid, mp 108–110 °C; $[\alpha]_D^{28}$ −38.7 (*c* 0.3, CH_3OH); ^1H NMR ($CDCl_3$) δ 3.42 (s, 3 H), 3.62 (m, 2H), 4.15 (d, *J* = 12.8 Hz, 2H), 4.59 and 4.92 (dd, *J* = 14.4, 14.8 Hz, 2H), 5.32 (m, 1H), 7.14 and 7.28 (s, 2H). IR (cm^{-1}): 3427, 1785, 1720, 1540, 1490, 1364, 1222, 1102, 839, 768, 599. HRMS (FAB) *m*/*z* (MH^+): calcd for $C_{10}H_{13}BrN_4O_6$, 365.0079; found, 365.0088.

4.6.5. TX-1880. Yield, 73% as a yellow solid, mp 135–136 °C; $[\alpha]_D^{28}$ +49.1 (*c* 0.3, CH_3OH); ^1H NMR ($CDCl_3$) δ 1.20 (s, 9 H), 3.50 and 3.60 (dd, *J* = 10.4 Hz, each 1H), 4.38 (d, *J* = 16.4 Hz, 2H) 4.59 and 4.92 (dd, *J* = 14.4, 14.6 Hz, 2H), 5.25 (m, 1H), 7.15 and 7.16 (s, 2H). IR (cm^{-1}): 3140, 1789, 1717, 1534, 1490, 1362, 1290, 1091, 841, 769, 636. Anal. Calcd for $C_{13}H_{19}ClN_4O_6$: C, 43.04; H, 5.28; N, 15.44. Found: C, 42.81; H, 5.06; N, 15.14.

4.6.6. TX-1881. Yield, 72% as a yellow solid, mp 135–136 °C; $[\alpha]_D^{28}$ −48.7 (*c* 0.4, CH_3OH); ^1H NMR ($CDCl_3$) δ 1.20(s, 9 H), 3.50 and 3.60 (dd, J=10.4 Hz, each 1H), 4.38 (d, J=16.0 Hz, 2H) 4.59 and 4.92 (dd, J=14.4, 14.6 Hz, 2H), 5.24 (m, 1H), 7.15 and 7.16 (s, 2H). IR (cm^{-1}): 3144, 1790, 1720, 1543, 1490, 1361, 1285, 1091, 1020, 836, 738, 632. Anal. Calcd for $C_{13}H_{19}ClN_4O_6$: C, 43.04; H, 5.28; N, 15.44. Found: C, 43.16; H, 5.20; N, 15.22.

4.6.7. TX-1882. Yield, 77% as a yellow solid, mp 141–142 °C; $[\alpha]_D^{28}$ +46.8 (*c* 0.2, CH_3OH); ^1H NMR ($CDCl_3$) δ 1.21 (s, 9 H), 3.52 and 3.60 (dd, J=10.6 Hz, each 1H), 4.21 (d, J=13.2 Hz, 2H) 4.59 and 4.87 (dd, J=14.6 Hz, 2H), 5.26 (m, 1H), 7.16 and 7.26 (s, 2H). IR (cm^{-1}): 3124, 1787, 1718, 1542, 1488, 1360, 1291, 1093, 842, 799, 698, 596. Anal. Calcd for $C_{13}H_{19}BrN_4O_6$: C, 38.34; H, 4.70; N, 13.76. Found: C, 38.12; H, 4.58; N, 13.60.

4.6.8. TX-1883. Yield, 74% as a yellow solid, mp 141–142 °C; $[\alpha]_D^{28}$ −49.4 (*c* 0.4, CH_3OH); ^1H NMR ($CDCl_3$) δ 1.20 (s, 9 H), 3.51 and 3.60 (dd, J=10.4, 10.6 Hz, each 1H), 4.21 (d, J=13.2 Hz, 2H) 4.59 and 4.87 (dd, J=14.6 Hz, 2H), 5.26 (m, 1H), 7.16 and 7.26 (s, 2H). IR (cm^{-1}): 3141, 1786, 1718, 1527, 1488, 1359, 1290, 1091, 840, 596. Anal. Calcd for $C_{13}H_{19}BrN_4O_6$: C, 38.34; H, 4.70; N, 13.76. Found: C, 38.35; H, 4.44; N, 13.73.

4.6.9. TX-1897. Yield, 95% as a yellow solid, mp 65–66 °C; $[\alpha]_D^{28}$ +51.6 (*c* 0.4, CH_3OH); ^1H NMR ($CDCl_3$) δ 1.30 (s, 9H), 4.17 and 4.18 (dd, J=4.4, 4.0 Hz, each 1H), 4.33 and 4.38 (d, J=15.6, 15.2 Hz, 2H), 4.74 and 5.04 (dd, J=14.4 Hz, 2H), 5.52 (m, 1H), 6.84 and 7.33 (dd, J=6.4, 6.8 Hz, 2H), 7.15 and 7.16 (d, J=0.8 Hz, 2H). IR (cm^{-1}): 3278, 2957, 1784, 1725, 1538, 1490, 1362, 1287, 1244, 1084, 838, 769, 651. Anal. Calcd for $C_{19}H_{23}ClN_4O_6$: C, 52.00; H, 5.28; N, 12.77. Found: C, 51.85; H, 5.37; N, 12.54.

4.6.10. TX-1899. Yield, 91% as a yellow solid, mp 66–67 °C; $[\alpha]_D^{28}$ −53.2 (*c* 0.2, CH_3OH); ^1H NMR ($CDCl_3$) δ 1.30 (s, 9H), 4.17 and 4.18 (dd, J=4.4, 4.0 Hz, each 1H), 4.35 and 4.36 (s, 2H), 4.74 and 5.04 (dd, J=14.8, 14.2 Hz, 2H), 5.52 (m, 1H), 6.84 and 7.34 (dd, J=2.2, 2.4 Hz, 2H), 7.15 and 7.16 (s, 2H). IR (cm^{-1}): 3278, 2957, 1789, 1725, 1544, 1490, 1362, 1287, 1244, 1084, 838, 769, 651. Anal. Calcd for $C_{19}H_{23}ClN_4O_6$: C, 52.00; H, 5.28; N, 12.77. Found: C, 51.81; H, 5.26; N, 12.49.

4.6.11. TX-1898. Yield, 98% as a yellow solid, mp 73–74 °C; $[\alpha]_D^{28}$ +53.7 (*c* 0.3, CH_3OH); ^1H NMR ($CDCl_3$) δ 1.30 (s, 9H), 4.15 and 4.18 (s, 1H), 4.20 and 4.23 (s, 2H), 4.74 and 5.04 (dd, J=14.8, 14.2 Hz, 2H), 5.52 (m, 1H), 6.84 and 7.33 (dd, J=6.8, 5.8 Hz, 2H), 7.15 and 7.17 (s, 1H). IR (cm^{-1}): 3278, 2957, 1784, 1720, 1538, 1490, 1362, 1287, 1244, 1084, 838, 774, 651, 555. Anal. Calcd for $C_{19}H_{23}BrN_4O_6$: C, 47.22; H, 4.80; N, 11.59. Found: C, 47.04; H, 4.73; N, 11.39.

4.6.12. TX-1900. Yield, 93% as a yellow solid, mp 74–75 °C; $[\alpha]_D^{28}$ −56.8 (*c* 0.3, CH_3OH); ^1H NMR ($CDCl_3$) δ 1.30 (s, 9H), 4.17 and 4.19 (d, J=5.2 Hz, 1H), 4.18 and 4.23 (s, 2H), 4.73 and 5.04 (d, J=14.8, 14.4 Hz, 2H), 5.53 (m, 1H), 6.84 and 7.33 (dd, J=6.8, 6.0 Hz, 2H), 7.15 and 7.17 (s, 1H). IR (cm^{-1}): 3139, 2957, 1784, 1720, 1538, 1490, 1362, 1287, 1244, 1084, 838, 774, 651, 555. Anal. Calcd for $C_{19}H_{23}BrN_4O_6$: C, 47.22; H, 4.80; N, 11.59. Found: C, 47.14; H, 4.68; N, 11.35.

Acknowledgements

This study was supported in part by the Japan–China Sasakawa Medical Fellowship. The author C.-Z.J. thanks 'The Japan–China Sasakawa Medical Fellowship', and also thanks Professor Shibata Shoji, Emeritus Professor of Tokyo University, for his helpful advice. The authors thank Dr. Goto Satoru of the Faculty of Pharmaceutical Sciences, The University of Tokushima, for his advice of Molecular modeling, and also Dr. Y. Takekawa, H. Nishitani, and Y. Nishimoto of the School of Medical, The University of Tokushima for their generous help with the radiobiological experiments. Thanks are also due to N. Mikamo, J. Azuma, A. Yokobori, K. Kiyoi of the Department of Biological Science and Technology for excellent technical assistance. We also thank M. Nakamura, E. Okayama, K. Yamashita of our faculty for performing the spectral measurements. We also thank DAISO Co., Ltd (Osaka, Japan) for providing (*R*)- and (*S*)-epichlorohydrin.

References and notes

1. Carmeliet, P.; Jain, R. K. *Nature* **2000**, *407*, 249.
2. Drevs, J.; Laus, C.; Medinger, M.; Schmidt-Gersbach, C.; Unger, C. *Onkologie* **2002**, *25*, 520.
3. Madhusudan, S.; Harris, A. L. *Curr. Opin. Pharmacol.* **2002**, *2*, 403.
4. Stopeck, A.; Sheldon, M.; Vahedian, M.; Cropp, G.; Gosalia, R.; Hannah, A. *Clin. Cancer Res.* **2002**, *8*, 2798.
5. Wedge, S. R.; Ogilvie, D. J.; Dukes, M.; Kendrew, J.; Chester, R.; Jackson, J. A.; Boffey, S. J.; Valentine, P. J.; Curwen, J. O.; Musgrove, H. L.; Graham, G. A.; Hughes, G. D.; Thomas, A. P.; Stokes, E. S.; Curry, B.; Richmond, G. H.; Wadsworth, P. F.; Bigley, A. L.; Hennequin, L. F. *Cancer Res.* **2002**, *62*, 4645.
6. Laird, A. D.; Christensen, J. G.; Li, G.; Carver, J.; Smith, K.; Xin, X.; Moss, K. G.; Louie, S. G.; Mendel, D. B.; Cherrington, J. M. *FASEB J.* **2002**, *16*, 681.
7. Ingber, D. E.; Fujita, T.; Kishimoto, S.; Kanamaru, T.; Sudo, K.; Brem, H.; Folkman, J. *Nature* **1990**, *348*, 555.
8. Kudelka, A. P.; Levy, T.; Verschraegen, C. F.; Edwards, C. L.; Piamsomboon, S.; Termrungruanglert, W.; Freedman, R. S.; Kaplan, A. L.; Kieback, D. G.; Meyers, C. A.; Jaeckle, K. A.; Loyer, E.; Steger, M.; Mante, R.; Mavligit, G.; Killian, A.; Tang, R. A.; Gutterman, J. U.; Kavanagh, J. J. *Clin. Cancer Res.* **1997**, *3*, 1501.
9. Hotz, H. G.; Reber, H. A.; Hotz, B.; Sanghavi, P. C.; Yu, T.; Foitzik, T.; Buhr, H. J.; Hines, O. J. *J. Gastrointest. Surg.* **2001**, *5*, 131.
10. Bhargava, P.; Marshall, J. L.; Rizvi, N.; Dahut, W.; Yoe, J.; Figuera, M.; Phipps, K.; Ong, V. S.; Kato, A.; Hawkins, M. J. *Clin. Cancer Res.* **1999**, *5*, 1989.
11. Harris, A. L. *Nat. Rev. Cancer* **2002**, *2*, 38.

12. Shimamura, M.; Nagasawa, H.; Ashino, H.; Yamamoto, Y.; Hazato, T.; Uto, Y.; Hori, H.; Inayama, S. *Br. J. Cancer* **2003**, *88*, 307.
13. Inomata, T.; Ogawa, Y.; Itoh, S.; Kariya, S.; Hamada, N.; Nishioka, A.; Yoshida, S.; Nagasawa, H.; Hori, H.; Inayama, S. *Int. J. Mol. Med.* **1999**, *4*, 257.
14. Abu-Zeid, M.; Hori, H.; Nagasawa, H.; Uto, Y.; Inayama, S. *Biol. Pharm. Bull.* **2000**, *23*, 190.
15. Abu-Zeid, M.; Hori, H.; Nagasawa, H.; Uto, Y.; Inayama, S. *Biol. Pharm. Bull.* **2000**, *23*, 195.
16. Abou-Bedair, F. A.; Hori, H.; Nagasawa, H.; Uto, Y.; Abu-Zeid, M.; Inayama, S. *Biol. Pharm. Bull.* **2002**, *25*, 591.
17. Kasai, S.; Nagasawa, H.; Yamashita, M.; Masui, M.; Kuwasaka, H.; Oshodani, T.; Uto, Y.; Inomata, T.; Oka, S.; Inayama, S.; Hori, H. *Bioorg. Med. Chem.* **2001**, *9*, 453.
18. Nagasawa, H.; Yamashita, M.; Mikamo, N.; Shimamura, M.; Oka, S.; Uto, Y.; Hori, H. *Comp. Biochem. Physiol. A Mol. Integr. Physiol.* **2002**, *132*, 33.
19. Hori, H.; Nagasawa, H.; Ishibashi, M.; Uto, Y.; Hirata, A.; Saijo, K.; Ohkura, K.; Kirk, K. L.; Uehara, Y. *Bioorg. Med. Chem.* **2002**, *10*, 3257.
20. Kasai, S.; Nagasawa, H.; Yamashita, M.; Masui, M.; Uto, Y.; Hori, H. *Bioorg. Med. Chem. Lett.* **2002**, *12*, 951.
21. Hori, H.; Jin, C.-Z.; Kiyono, M.; Kasai, S.; Shimamura, M.; Inayama, S. *Bioorg. Med. Chem.* **1997**, *5*, 591.
22. Edwards, D. I. *J. Antimicrob. Chemther.* **1993**, *31*, 9.
23. Naylor, M. A.; Threadgill, M. D.; Hollis Showalter, H. D.; Stratford, I. J.; Stephens, M. A.; Fielden, E. M.; Adams, G. E. *Drug Des. Discov.* **1993**, *10*, 249.
24. Mah-Becherel, M. C.; Ceraline, J.; Deplanque, G.; Chenard, M. P.; Bergerat, J. P.; Cazenave, J. P.; Klein-Soyer, C. *Br. J. Cancer* **2002**, *86*, 803.
25. Apers, S.; Paper, D.; Burgermeister, J.; Van Dyck, S.; Lemiere, G.; Vlietinck, A.; Pieters, L. *J. Nat. Prod.* **2002**, *65*, 718.
26. Ban, F.; Gauld, J. W.; Boyd, R. J. *J. Am. Chem. Soc.* **2001**, *123*, 7320.
27. Jin, C.-Z.; Quan, Z.-S.; Hori, H. *Chin. J. Med. Chem.* **1999**, *9*, 21.
28. Shibamoto, Y.; Ono, K.; Takahashi, H.; Kano, E.; Hori, H.; Shibata, T.; Inayama, S.; Abe, M. *Jpn. J. Cancer Res.* **1986**, *77*, 1027.
29. Dupuy, E.; Habib, A.; Lebret, M.; Yang, R.; Levy-Toledano, S.; Tobelem, G. *J. Thromb. Haemost.* **2003**, *1*, 1096.
30. Cher, M. L.; Biliran, H. R., Jr.; Bhagat, S.; Meng, Y.-H.; Che, M.-X.; Lockett, J.; Abrams, J.; Fridman, R.; Zachareas, M.; Sheng, S. J. *Proc. Natl. Acad. Sci. U.S.A.* **2003**, *100*, 7847.
31. Pennacchietti, S.; Michieli, P.; Galluzzo, M.; Mazzone, M.; Giordano, S.; Comoglio, P. M. *Cancer Cell* **2003**, *3*, 347.
32. Mosman, T. *J. Immunol. Meth.* **1983**, *65*, 55.
33. Oikawa, T.; Shimamura, M.; Ashino, H.; Nakamura, O.; Kanayasu, T.; Morita, I.; Murota, S. *J. Antibiot.* **1992**, *45*, 1155.
34. Hori, H.; Yokoyama, H.; Murayama, C.; Mori, T.; Yonei, S.; Satoh, T.; Inayama, S. *Biol. Pharm. Bull.* **1992**, *17*, 1676.
35. Sin, N.; Meng, L.; Wang, M. Q. W.; Wen, J. J.; Bornmann, W.; Crews, C. M. *Proc. Natl. Acad. Sci. U.S.A.* **1997**, *94*, 6099.
36. Griffith, E. C.; Su, Z.; Turk, B. E.; Chen, S.; Chang, Y. H.; Wu, Z.; Biemann, K.; Liu, J. O. *Chem. Biol.* **1997**, *4*, 461.
37. Griffith, E. C.; Su, Z.; Niwayama, S.; Ramsay, C. A.; Chang, Y. H.; Liu, J. O. *Proc. Natl. Acad. Sci. U.S.A.* **1998**, *95*, 15183.
38. Liu, S.; Widom, J.; Kemp, C. W.; Crews, C. M.; Clardy, J. *Science* **1998**, *282*, 1324.
39. Wang, J.; Sheppard, G. S.; Lou, P.; Kawai, M.; BaMaung, N.; Erickson, S. A.; Tucker-Garcia, L.; Park, C.; Bouska, J.; Wang, Y. C.; Frost, D.; Tapang, P.; Albert, D. H.; Morgan, S. J.; Morowitz, M.; Shusterman, S.; Maris, J. M.; Lesniewski, R.; Henkin, J. *Cancer Res.* **2003**, *63*, 7861.
40. Farrant, E.; Mann, J. *J. Chem. Soc. Perkin Trans. 1* **1997**, *3*, 1083.
41. Enholm, E. J.; Jiang, S. *J. Org. Chem.* **2000**, *65*, 4756.
42. Keezer, S. M.; Ivie, S. E.; Krutzsch, H. C.; Tandle, A.; Libutti, S. K.; Roberts, D. D. *Cancer Res.* **2003**, *63*, 6405.
43. Kim, D. J.; Min, J. K.; Ahn, S. K.; Lee, H. W.; Choi, N. S.; Moon, S. K. *Chem. Pharm. Bull.* **2004**, *52*, 447.
44. Satchi-Fainaro, R.; Puder, M.; Davies, J. W.; Tran, H. T.; Sampson, D. A.; Greene, A. K.; Corfas, G.; Folkman, J. *Nat. Med.* **2004**, *10*, 255.